

The effect of partial substitution on the hydroxyapatite properties

Lenka Šimková* and Petra Šulcová

*Department of Inorganic Technology, The University of Pardubice,
CZ–532 10 Pardubice, Czech Republic*

Received: May 5, 2020; Accepted: May 25, 2020

The aim of this research was the synthesis of hydroxyapatite powders of the $(Ca_{10}(PO_4)_6(OH)_2)$ type by a precipitation method with the following synthesis conditions: the ratio of $Ca/P = 1$, $pH\ 7$). Another main target of this work was a partial substitution of calcium in the hydroxyapatite structure with selected doping elements (magnesium, zinc, aluminium, strontium) with the subsequent assessment of the effect of such replacements on the structure and physicochemical properties of hydroxyapatite. The synthesized powders were characterized by X-ray diffraction (XRD), in order to identify the phase composition and crystallinity, and by scanning electron microscopy (SEM) to study the morphology of synthesized powder. Finally, to define the anticorrosive purposes, preliminary corrosion tests were also performed.

Keywords: Hydroxyapatite; Co–substitution; XRD; SEM; Corrosion tests

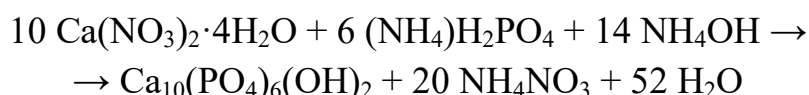
Introduction

The hydroxyapatite $[Ca_{10}(PO_4)_6(OH)_2; HAP]$ is the very common phosphate apatite which has been considerably investigated from an experimental point of view due to its appreciable biotechnological, technological and industrial features [1,2]. The general formula for apatite compounds is $M_{10}(XO_4)_6Z_2$. Its crystal structure (monoclinic and hexagonal) is capable of cationic ($M = Ba^{2+}, Sr^{2+}, Mg^{2+}, Zn^{2+}$, etc. [3]) and/or anionic ($Z = F^-, Br^-, Cl^-, OH^-; X = As, Si$ [4,5]) substitutions, altering both biological and physical properties [6–8]. In accordance with this statement, various forms of the substituted apatites have been proposed for

* Corresponding author, ✉ lenka.simkova1@student.upce.cz

biomedical applications that include identification and determination of natural impurities in bone tissues (Na^+ , Mg^{2+} , Sr^{2+} , CO_3^{2-} , F^- and SiO_3^{2-}), increasing the structural defects in hydroxyapatite and affecting also its solubility [9,10]. Hydroxyapatite is used as a protective coating of metal prostheses in the human body having two important functions; namely, to protect the incorporated material against corrosion and to improve the acceptability and inertness of the implant for the human body [11]. Since hydroxyapatite is especially convenient for defending the implant against corrosion, in terms of physicochemical and structural properties, this can also be very functional for steel protection (as with other phosphate compounds) [12].

Hydroxyapatite can be synthesized by using a number of different methods, like those based on reactions in the solid state [13], co-precipitation [14,15], hydrothermal methods [16], the sol-gel process [17,18], microwave processing [19], and others [20]. The most common method is co-precipitation from water solutions, under certain conditions, when crystallites of insoluble hydroxyapatite are formed [20]. In the co-precipitation method are two types of processes, the most common being the reaction of calcium and phosphate salts (described in this paper) [21]



In the previous study [22], the effect of precipitation conditions on hydroxyapatite synthesis and structure has already been demonstrated. Based on these results, the following synthesis conditions were selected for this research: $\text{Ca}/\text{P} = 1$, $\text{pH} = 7$ and precipitation rate = 2 mL min^{-1} . The work presented herein is focused on partial substitution of the calcium ions by other selected ones in the structure of hydroxyapatite and on characterization of the altered structure and of their properties. The synthesized powders were evaluated in terms of the phase composition, crystal size, morphology, and anticorrosive purposes.

Materials and methods

Synthesis of pure and doped hydroxyapatite powders

For selecting the convenient synthesis conditions for the formation of pure and doped HAP phase, the thermodynamic stability of pure HAP in aqueous solution was analyzed and implemented under laboratory conditions.

Subsequently, the selected precipitation conditions, which means Ca/P ratio, range of pH and precipitation speed, were applied in the synthesis of doped HAP (see Table 1, precipitation speed 2 mL min^{-1}). For the synthesis of the samples, 1 mol L^{-1} solutions of the original compounds ($\text{Ca}(\text{NO}_3)_2 \cdot 4\text{H}_2\text{O}$, $\text{Al}(\text{NO}_3)_3 \cdot 9\text{H}_2\text{O}$, $\text{Mg}(\text{NO}_3)_2 \cdot 6\text{H}_2\text{O}$, $\text{Zn}(\text{NO}_3)_2 \cdot 6\text{H}_2\text{O}$, $\text{Sr}(\text{NO}_3)_2$, $(\text{NH}_4)\text{H}_2\text{PO}_4$), all from Lachema,

Brno, Czech Republic, Sigma-Aldrich, Steinheim, Germany, purity >98 %) were prepared. The exact concentration of these solutions was determined by analytical methods (titration, photometric and gravimetric analyses [22,23]). The obtained powders were left to age for one day, then filtered and washed with distilled water to neutral pH and dried at 80 °C for 6 h. The synthesized powders were further assessed in terms of their phase composition (XRD, MiniFlex 600, Rigaku, Tokyo, Japan), the morphology of samples (SEM, LYRA 3, Tescan, Brno, Czech Republic), and corrosion inhibition (preliminary corrosion tests).

Table 1 Overview of the obtained samples and the conditions of synthesis

Sample	Composition	(Ca + M)/P
1	Ca ₁₀ (PO ₄) ₆ (OH) ₂	1
1-Mg	Ca _{9.5} Mg _{0.5} (PO ₄) ₆ (OH) ₂	1
1-Zn	Ca _{9.5} Zn _{0.5} (PO ₄) ₆ (OH) ₂	1
1-Sr	Ca _{9.5} Sr _{0.5} (PO ₄) ₆ (OH) ₂	1
1-Al	Ca _{9.25} Al _{0.5} (PO ₄) ₆ (OH) ₂	0.975 *

* Due to the presence of trivalent Al^{III}

Characterization of pure and doped hydroxyapatite phases

The phase analysis of the samples was identified by X-ray diffraction analysis using MiniFlex-600 diffractometer equipped with a vertical goniometer of 17 cm in the 2θ range of 10–50°. The accuracy of goniometer was ±0.02°. X-ray tube with Cu-anode was used ($U = 40$ kV, $I = 15$ mA, CuKα radiation).

The morphology of the powders was studied by scanning electron microscope equipped with EDS analyzer AZtec X-Max 20 (Oxford Instruments, Concord, MA, USA) at an acceleration voltage of 20 kV. The resulting image was formed by the secondary signal – reflected or secondary electrons.

In terms of behaving as the corrosion inhibitor, preliminary corrosion tests were executed, including the determination of pH and resistivity of aqueous suspensions of pigments (10 %, w/w), gravimetric determination of weight loss of the steel plates and determination of corrosion indicators for steel plates.

Results and discussion

Effect of partial substitution on the structure and properties of HAP

The phase composition of the prepared samples was determined by XRD analysis. Two different structures of hydroxyapatite have been identified: (i) monoclinic and (ii) hexagonal. Almost all samples showed a single-phase composition but

only one doped sample (1-Mg) revealed two phases: hydroxyapatite $\text{Ca}_{10}(\text{PO}_4)_6(\text{OH})_2$ and whitlockite $\text{Ca}_{18}\text{Mg}_2\text{H}_2(\text{PO}_4)_{14}$ (see Fig. 1 and Table 2). Since only the HAP phase has been identified in other doped samples, it is clear that doping ions (Mg^{2+} , Zn^{2+} , Al^{3+} , and Sr^{2+}) occupy the calcium positions in the crystal structure of HAP. This can be expected because the ionic radii of these elements are approximately the same or smaller than the radius of Ca ($r_{\text{Ca}^{2+}} = 0.11$ nm, $r_{\text{Mg}^{2+}} = 0.072$ nm, $r_{\text{Zn}^{2+}} = 0.074$ nm, $r_{\text{Al}^{3+}} = 0.054$ nm, $r_{\text{Sr}^{2+}} = 0.13$ nm).

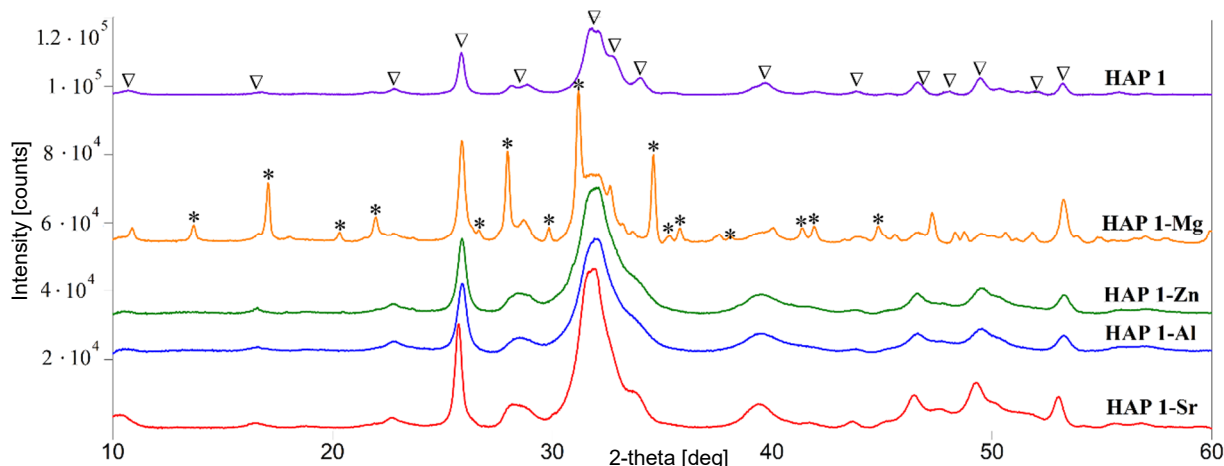


Fig. 1 X-ray diffraction patterns of pure and doped hydroxyapatite phases

Table 2 The phase composition of identified hydroxyapatite phases

Sample/HAP	Chemical formula	Identified phases
1	$\text{Ca}_{10}(\text{PO}_4)_6(\text{OH})_2$	$\text{Ca}_{10}(\text{PO}_4)_6(\text{OH})_2$ (▽, hydroxyapatite)
1-Mg	$\text{Ca}_{9.5}\text{Mg}_{0.5}(\text{PO}_4)_6(\text{OH})_2$	$\text{Ca}_{10}(\text{PO}_4)_6(\text{OH})_2$, $\text{Ca}_{18}\text{Mg}_2\text{H}_2(\text{PO}_4)_{14}$ (*, whitlockite)
1-Zn	$\text{Ca}_{9.5}\text{Zn}_{0.5}(\text{PO}_4)_6(\text{OH})_2$	$\text{Ca}_{10}(\text{PO}_4)_6(\text{OH})_2$
1-Sr	$\text{Ca}_{9.5}\text{Sr}_{0.5}(\text{PO}_4)_6(\text{OH})_2$	$\text{Ca}_{10}(\text{PO}_4)_6(\text{OH})_2$
1-Al	$\text{Ca}_{9.25}\text{Al}_{0.5}(\text{PO}_4)_6(\text{OH})_2$	$\text{Ca}_{10}(\text{PO}_4)_6(\text{OH})_2$

A comparison of the crystal size gained from SEM and XRD analysis had indicated that the minimum dimensions from SEM analysis were comparable to the maximum dimensions from that by XRD. In general, the SEM analysis has shown bigger particles, which can be explained by the fact that for the maximum crystal size analysis the largest particles visible in the SEM images are selected (Fig. 2). The contribution of these largest particles to the average crystal size is nevertheless small. Yet another interpretation can be that the largest crystals visible in SEM images are, in fact, agglomerates of smaller crystals.

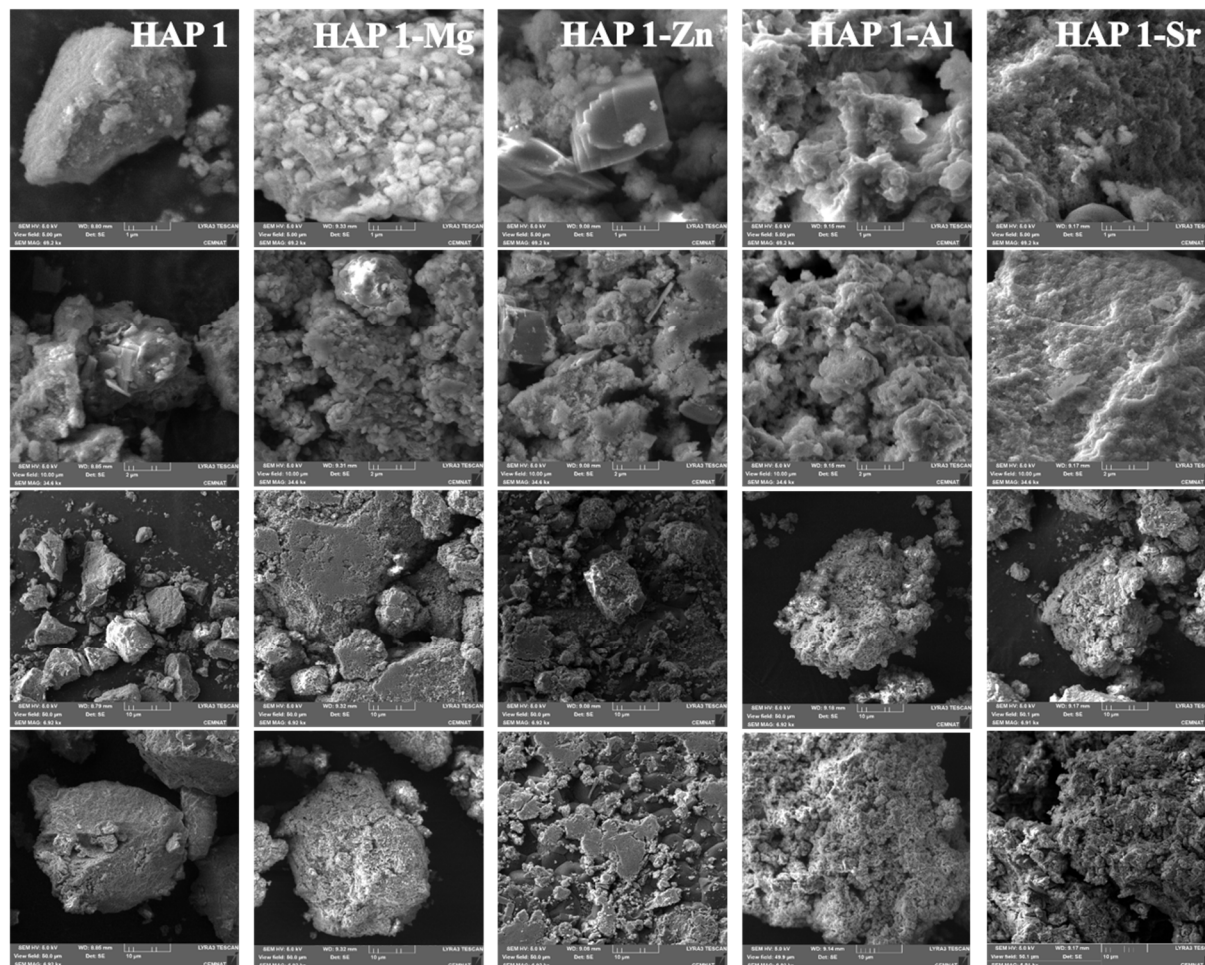


Fig. 2 SEM scans of pure and doped HAP samples

Effect of substitution on the corrosion efficiency of HAP

Preliminary corrosion tests included the determination of pH and resistance of aqueous suspensions of the respective pigments (10 %), gravimetric determination of weight loss of steel plates and determination of corrosion indicators for steel plates.

The measurement of pH and resistivity of aqueous suspensions of pigments aimed us to simulate the working conditions of the pigments studied. The value of pH in the range of 7–9 is considered optimal for effective inhibition of corrosion, but in the case of phosphate-based anti-corrosion pigments, slightly acidic pH values could also be used. The conductivity values have suggested us the concentration of dissociated species formed as a result of the hydrolysis and may attend in the corrosion inhibition processes. Fig. 3 demonstrates the change in the pH value and conductivity of the pigment suspension during a period of 28 days.

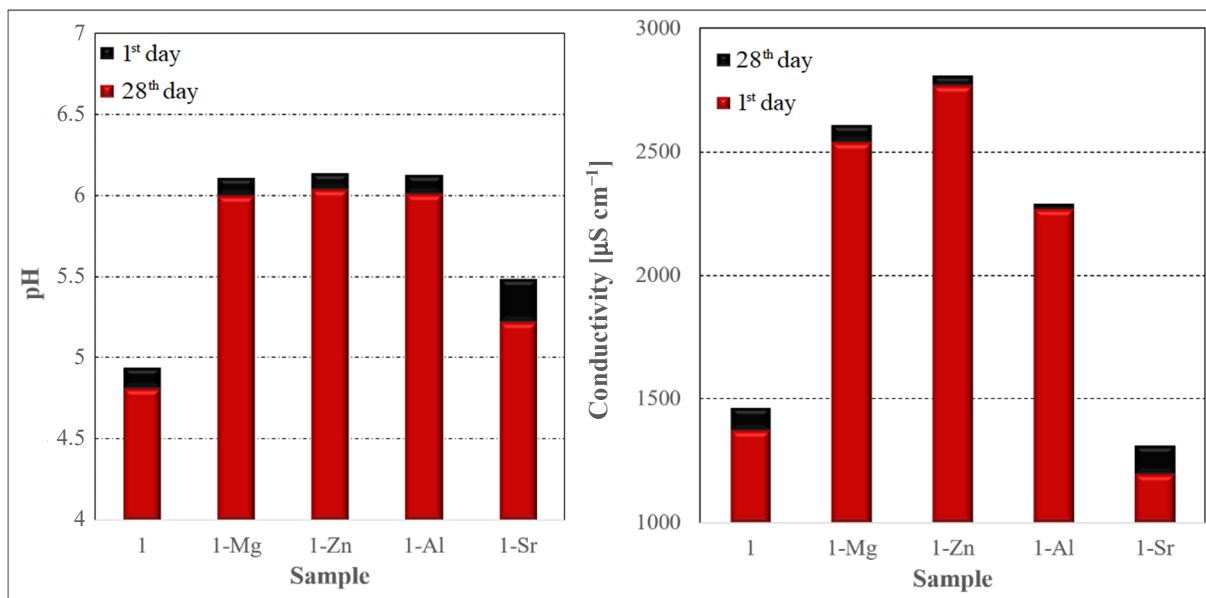


Fig. 3 Results of preliminary corrosion tests: change of the pH and conductivity of the pigment suspensions during 28 days of aging

Based on the values obtained from the preliminary corrosion tests, it has been shown that hydrolysis of pigment ions favors the formation of acid species, resulting in a decrease of pH. The conductivity of the samples was very different, but in general, it increased indicating that the concentration of dissociated ions has increased over time. The aqueous suspensions of the pigments were filtered and the pigments extracts used for the assessment of weight loss of steel plates immersed during 2 months. During the test, a remarkable color change of the extracts was observed being apparently due to the release of corrosion products (rust). Next, corrosion indicators were calculated on the basis of corrosion losses of steel plates (Fig. 4).

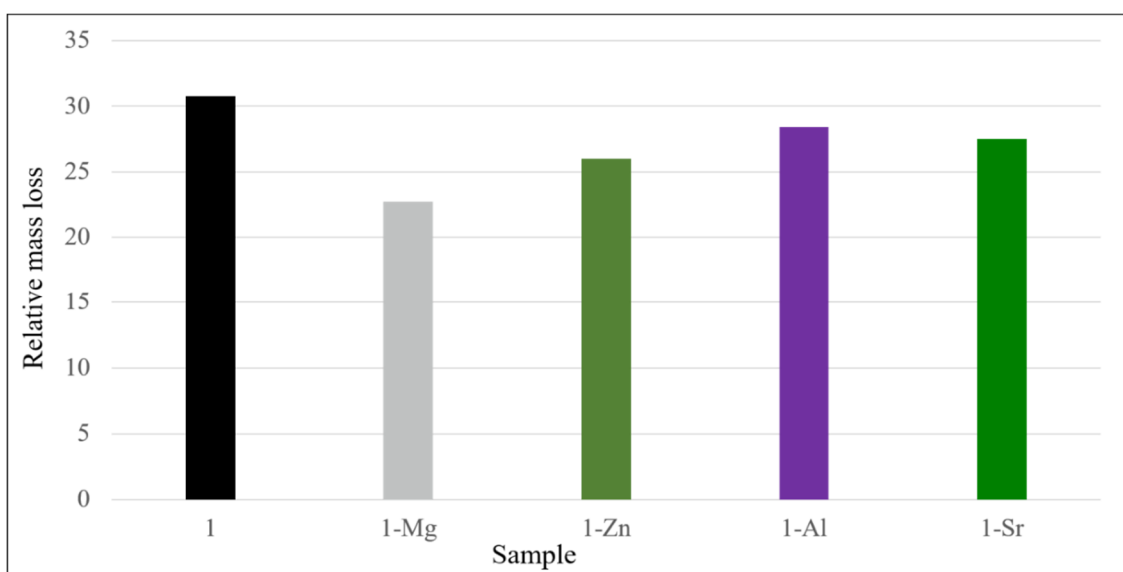


Fig. 4 Results of the preliminary corrosion tests: relative decrease of weight of the samples

Based on the values of corrosion indicators of the measured samples, it is possible to select samples with high anticorrosion efficiency, which is enabled by sufficient concentration of phosphates in the extracts, forming a protective coating (chemically: vivianite, $\text{Fe}_3(\text{PO}_4)_2 \cdot 4\text{H}_2\text{O}$) on the surface of steel plates.

Conclusions

The selected conditions for synthesis (Ca/P ratio = 1 and pH = 7) have been found suitable for the formation of pure and doped hydroxyapatite phases.

From the results of XRD analysis, it is clear that two distinct structures of hydroxyapatite have been identified: (i) monoclinic and (ii) hexagonal. Only for one doped sample (1-Mg), two different phases (hydroxyapatite and whitlockite) have been identified in the phase composition. Thus, in other cases, the selected elements (Zn, Al, Sr) partially occupy the positions of calcium in the crystal structure of HAP. These structural types of hydroxyapatite were selected based on the lowest value of FOM (“Figure Of Merit”), i.e., based on the best match.

From the SEM images, it is evident that the particles of doped samples are slightly smaller than those for pure HAP and the minimum values of crystal size observed by this method comparable with the maximum values according to XRD analysis.

Preliminary corrosion tests have then revealed that hydrolysis of pigment ions favors the formation of acid species resulting in a lower pH and the increase of conductivity values. By the corrosion indicators, the samples can be classified according to their anticorrosion efficiency into a group with high corrosion efficiency (Vivianite, $\text{Fe}_3(\text{PO}_4)_2 \cdot 4\text{H}_2\text{O}$, as protective coating).

From the previous study [22], the most satisfactory results were demonstrated for the sample 1 (Ca/P = 1, pH = 7; the smallest particles, thin needles, the narrowest range of particle size, space group P63/m, products β -TCP, and T-TPC) and this is the reason, why just this sample could be doped by selected elements (Mg, Zn, Al, and Sr).

Acknowledgments

This work has been supported by University of Pardubice under the project SGS_2020_008. The authors appreciate a financial support from the Ministry of Education, Youth and Sports of the Czech Republic (grant LM2015082) and from European Regional Development Fund (project “Modernization and Upgrade of the CEMNAT”; CZ.02.1.01/0.0/0.0/16_013/0001829).

References

- [1] Slepko A., Demkov A.A.: First-principles study of the biomineral hydroxyapatite. *Physical Review B* **84** (2011) 134108–134118.
- [2] Yaemsunthorn K., Randorn C.: Hydrogen production using economical and environmental friendly nanoparticulate hydroxyapatite and its ion doping. *International Journal of Hydrogen Energy* **42** (2017) 5056–5062.
- [3] Shepherd J.H., Shepherd D.V., Best S.M.: Substituted hydroxyapatites for bone repair. *Journal of Material Science: Materials in Medicine* **23** (2012) 2335–2347.
- [4] Stanić V., Dimitrijević S., Antonović D.G., Jokić B.M., Zec S.P., Tanasković S.T., Raičević S.: Synthesis of fluorine substituted hydroxyapatite nanopowders and application of the central composite design for determination of its antimicrobial effects. *Applied Surface Science* **290** (2014) 346–352.
- [5] Merry J.C., Gibson I.R., Best S.M., Bonfield W.: Synthesis and characterization of carbonate hydroxyapatite. *Journal of Material Science: Materials in Medicine* **9** (1998) 779–783.
- [6] Zilm M., Chen L., Sharma V., McDannald A., Jain M., Ramprasad R.: Hydroxyapatite substituted by transition metals: Experiment and theory. *Physical Chemistry Chemical Physics* **18** (2016) 16457–16465.
- [7] Supova M.: Substituted hydroxyapatites for biomedical applications: A review. *Ceramics International* **41** (2015) 9203–9231.
- [8] Wang M., Wang Q., Lu X., Wang K., Ren F.: Computer simulation of ions doped hydroxyapatite: A brief review. *Journal of Material Science* **32** (2017) 978–987.
- [9] Boanini E., Gazzano M., Bigi A.: Ionic substitutions in calcium phosphates synthesized at low temperature. *Acta Biomaterialia* **6** (2010) 1882–1894.
- [10] Cacciotti I.: *Handbook of bioceramics and biocomposites: Cationic and anionic substitutions in hydroxyapatite*. Springer, Cham 2015.
- [11] Huang Y., Hao M., Nian X., Qiao H., Zhang X., Zhang X., Song G., Guo J., Pang X., Zhang H.: Strontium and copper co-substituted hydroxyapatite-based coatings with improved antibacterial activity and cytocompatibility fabricated by electrodeposition. *Ceramics International* **42** (2016) 11876–11888.
- [12] Gorodylova N., Dohnalová Ž., Šulcová P., Bělina P., Vlček M.: Influence of synthesis conditions on physicochemical parameters and corrosion inhibiting activity of strontium pyrophosphates $\text{SrM}^{\text{II}}\text{P}_2\text{O}_7$ ($\text{M}^{\text{II}} = \text{Mg}$ and Zn). *Progress in Organic Coating* **93** (2016) 77–86.
- [13] Arita I.H., Castano V.M., Wilkinson D.S.: Synthesis and processing of hydroxyapatite ceramic tapes with controlled porosity. *Journal of Materials Science* **6** (1995) 19–23.
- [14] Akao M., Aoki H., Kato K.: Mechanical properties of sintered hydroxyapatite for prosthetic applications. *Journal of Materials Science* **16** (1981) 809–812.
- [15] Kong L.B., Ma J., Boey F.: Nanosized hydroxyapatite powders derived from coprecipitation process. *Journal of Materials Science* **37** (2002) 1131–1134.
- [16] Zhang X., Vecchio K.S.: Hydrothermal Synthesis of Hydroxyapatite Rods. *Journal of Crystal Growth* **308** (2007) 133–140.
- [17] Wang J., Shaw L.L.: Synthesis of high purity hydroxyapatite nanopowder via sol-gel combustion process. *Journal of Materials Science* **20** (2009) 1223–1227.

- [18] Jilavenkatesa A.: Sol-gel processing of hydroxyapatite. *Journal of Materials Science* **33** (1998) 4111–4119.
- [19] Yang Y., Ong J.L., Tian J.: Rapid sintering of hydroxyapatite by microwave processing. *Journal of Materials Science Letters* **21** (2002) 67–69.
- [20] Safronova T.V., Shekhirev M.A., Putlyayev V.I.: Ceramics Based on Calcium Hydroxyapatite Synthesized in the Presence of PVA. *Glass and Ceramics* **64** (2007) 408–412.
- [21] Vazquez C.G., Barba C.P., Munguia N.: Stoichiometric hydroxyapatite obtained by precipitation and sol-gel processes. *Revista Mexicana de Fisica* **51** (2005) 284–293.
- [22] Šimková L., Gorodylova N., Dohnalová Ž., Šulcová P.: Influence of precipitation conditions on the synthesis of hydroxyapatite. *Ceramics-Silikáty* **62** (2018) 253–260.
- [23] Přibil R.: *Complexometry* (in Czech). SNTL, Prague 1961.